IEEE Access
Multidisciplinary ⋮ Rapid Review ⋮ Open Access Journal

Received August 26, 2017, accepted September 28, 2017, date of publication October 13, 2017, date of current version November 14, 2017.

Digital Object Identifier 10.1109/ACCESS.2017.2762665

INVITED PAPER

Adaptive Repetitive Control of Hydraulic Load Simulator With RISE Feedback

CHENGYANG LUO[1], JIANYONG YAO[1,2], FUHONG CHEN[3], LAN LI[4], AND QIANG XU[1]

[1]School of Mechanical Engineering, Nanjing University of Science and Technology, Nanjing 210094, China
[2]Hebei Provincial Key Laboratory of Heavy Machinery Fluid Power Transmission and Control, Qinhuangdao 066004, China
[3]Seventh Design Department, Aerospace Science and Technology Corporation, Seventh Research Institute, Chengdu 610100, China
[4]Beijing Institute of Space Launch Technology, Beijing 100076, China

Corresponding author: Jianyong Yao (jerryyao.buaa@gmail.com)

This work was supported in part by the National Natural Science Foundation of China under Grant 51675279, in part by the Postgraduate Cultivation Innovation Project of Jiangsu province under Grant KYZZ16_0197, in part by the Natural Science Foundation of Jiangsu province under Grant BK20170035, in part by the Hebei Provincial Key Laboratory of Heavy Machinery Fluid Power Transmission and Control under Grant HBSZKF2016-1, and in part by the China Academy of Launch Vehicle Technology University Joint Innovation Fund under Grant CALT201605.

ABSTRACT Electro-hydraulic load simulator is a typical test-equipment for hardware-in-the-loop simulation, and usually performs periodic tasks, in which the modeling uncertainties will also present some periodicity. With this notification, in this paper, the system model of electro-hydraulic load simulator is established, afterward, all periodic uncertainties are transformed into linear-in-parameters form by applying Fourier series approximation, then an adaptive repetitive scheme with a robust integral of the sign of the error (RISE) feedback is synthesized, in which adaptive repetitive law is designed to handle periodic uncertainties and RISE robust term to attenuate unmodeled disturbances. The developed controller features depending on the desired trajectory rather than the system states, therefore it requires little information of the dynamic system and uncertain nonlinearities, which can apparently restrain the problems from noise pollution. In addition, because the periodic uncertainties are approximated as Fourier series and then compensated, the system performance can be greatly improved when performing periodic tasks. The resulting final control input is continuous while asymptotic tracking performance can be achieved with various uncertainties and disturbances by the proposed controller via Lyapunov stability analysis. In comparison to the other three controllers, the effectiveness and high performance of the proposed control method are validated by the experimental results sufficiently.

INDEX TERMS Adaptive control, repetitive control, RISE robust control, electro-hydraulic load simulator, force control.

I. INTRODUCTION

Electro-hydraulic load simulator (EHLS), which can simulate the air load on positioning actuation system of aircraft, is a necessary experimental platform in aviation and aerospace field [1]–[4]. The most troublesome problem when developing a high-performance EHLS is that the motion disturbance of aircraft actuator will severely affect the control performance because EHLS and the positioning actuator system are connected directly by a stiff structure. Typically, the force caused by the actuation movement is called the extraneous force. Hence, increasing attention is attracted to alleviate the effect of extraneous force and improve the tracking performance of EHLS.

Displacement/velocity synchronization is an effective method which is widely employed to eliminate the extraneous force by using an accessional hydraulic motor in practical implementation. On the basis of the conventional proportional-integral-derivative (PID) controller, Jiao, et al. researched the reasons and sources of disturbance between EHLS and the hydraulic aircraft actuator and proposed the PID controller with velocity synchronization (VPID) [2]. Although VPID is easily affected by the velocity synchronization accuracy of actuator and EHLS, its ability of disturbance-rejection is apparently enhanced in comparison to the PID controller. In addition to VPID, many feed-forward compensation strategies are employed to reduce the extraneous force [4]. Furthermore, many other control strategies such as adaptive robust control (ARC) [5], fuzzy PID control [6] and neutral network control with learning vector quantization [7] are also developed to improve the control performance of EHLS.

In practice, electro-hydraulic load simulator is usually required to perform complex tasks, where one kind is periodic and another is non-periodic. Though the closed-loop stability can be guaranteed by the aforementioned control method, perfect tracking performance may be difficult to be achieved, especially for the periodic tasks. Aiming at improving the tracking capability when performing periodic tasks, the concept of repetitive control [8] is then introduced by changing the control input according to the characteristic of system control error. However, what the conventional repetitive learning algorithm does is equivalent to adapting all the values of the periodic uncertainties in a cycle, hence the conventional repetitive controllers are easily effected by the pollution of noise, which is a huge obstacle for them to be utilized in many implementations [8]–[11]. In order to enhance the stability and reliability of the repetitive controller with the effects by noise, Q filters [12] are considered in the internal model and achieve obvious improvement. In [13], the repetitive control strategy is utilized in ripple eliminators and successfully enhanced the power quality of DC systems.

However, the aforementioned repetitive control methods [10]–[13] are failed to solve the parametric uncertainties and unmodeled disturbances, which gradually become the primary obstacles of pursuing higher tracking performance. Typically, adaptive control can effectively overcome parametric uncertainties and enhance the tracking capability by estimating the unknown but constant parameters. In [14], [15], Yao and Tomizuka developed adaptive robust control (ARC), which provides a novel and intelligent thinking for the designs of new effective control schemes to utilize the adaptive control and robust control [16]–[18]. Moreover, an ARC scheme is developed in [5] for the nonlinear system model of EHLS. Although ARC was applied in many applications [5], [10], [14], [15], [19], [20], it depends on the correct model of the system dynamic information, which means that the potential parametric uncertainties and unmodeled disturbance may degrade the performance or even affect the stability of the system. In addition, it is noticeable that when EHLS performs periodic command, the parametric uncertainties will also show the periodicity. Therefore, to deal with this problem for repetitive control, adaptive robust repetitive control schemes are developed in [10] and [21], in which less parameters are adapted and the noise sensitive problem is dealt with. However, although [10], [21] can handle the periodic modeling uncertainties by applying Fourier series approximation, the system parametric uncertainties are ignored, which gradually become the main obstacles of pursuing higher tracking performance [22], [23]. Furthermore, because the Fourier series cannot completely represent the unmodeled uncertainties, the remaining error may be a potential factor which will affect the tracking performance.

Robust control is an effective tool to enhance the disturbance-rejection ability of the closed-loop system against unmodeled dynamic, however in some cases, conventional robust control might become a kind of high-gain feedback, especially when confronted with the modeled systems only with the parametric uncertainties. Although the adaptive robust control is widely utilized, it can just achieve bounded tracking performance. In [24], a new robust feedback control approach, namely the robust integral of the sign of the error (RISE), was proposed by B. Xian. When the matched unmodeled disturbances are smooth enough, then the asymptotic tracking performance can be obtained [25]–[27]. Reference [28] proposed a RISE-based robust adaptive control method with the compensation of the unknown state delays and finally obtained asymptotic tracking results. References [29] and [30] designed a RISE-based saturated control scheme for a class of uncertainty, which can utilize the advantages of high-gain controller as long as the saturation is within the limits. The conclusions in [24]–[30] demonstrate that the RISE feedback term can effectively enhance the transient tracking capability and decrease the steady-state error. In addition, to handle the parametric uncertainties and unmodeled disturbances effectively [31], Yao proposed an adaptive compensation scheme with RISE feedback for high accuracy tracking control to cope with both payload and unknown system parameters synchronously. However, though performing periodic tasks, it is regretful that the periodicity of unmodeled uncertainties and disturbances is ignored.

In this paper, in order to overcome the difficulties in repetitive control tasks for EHLS, a practical adaptive repetitive controller with RISE feedback is synthesized, considering all the parameters concerned to be unknown. Through the control method proposed in this paper, the periodicity is exploited and then the state-dependent unmodeled uncertainties are transformed into some basis functions via Fourier series. Consequently, these unmodeled uncertainties can be easily solved as long as the amplitudes of the basis functions are adapted correctly. Finally, the designed method presents an asymptotic tracking performance in the presence of both periodic-like unmodeled disturbances and parametric uncertainties meanwhile results in a continuous control effort. In addition to the great tracking performance, some practical benefits are also important, such as lower noise-sensitivity and less memory occupation [10], [21]. Effectiveness and feasibility of EHLS for asymptotic tracking capability are then verified by theoretical analysis and extensive comparative experimental results.

The rest parts of this paper are arranged as follows. Problem formulation and dynamic models are obtained in Section II. Section III presents the adaptive repetitive RISE controller design procedure and its theoretical results. Comparative experimental results and analysis are given in Section IV. Section V presents the conclusions.

II. PROBLEM FORMULATION AND DYNAMIC MODELS

Fig. 1 shows the structure of aircraft actuator system and electro-hydraulic load simulator. The left part of Fig. 1 is the loaded aircraft actuator system while the right part is electro-hydraulic load simulator. The aircraft actuator can drive the aircraft control surface which is simulated by the

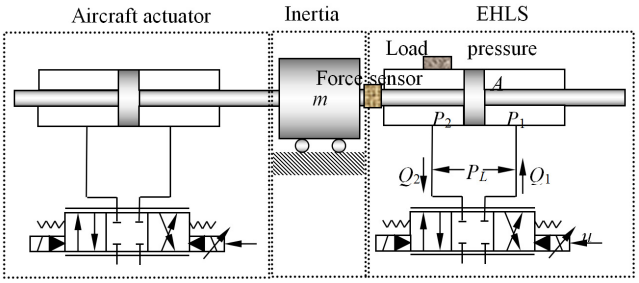

FIGURE 1. The architecture of the electro-hydraulic load simulator.

inertia load. With the movement of the left part, the right part will be affected directly because of the stiffness connection. The main functions of EHLS are proving the stability and performance of the aircraft actuation systems before the actual flight and future airborne operation [5], [18].

The force output of force sensor mounted on EHLS can be written by [5]

$$T = AP_L - B\dot{y} - f(t, y, \dot{y}) \tag{1}$$

where T is force output, A is displacement of loading hydraulic actuator, $P_{\mathrm{L}} = P_1$-P_2 is load pressure between the two chambers of the actuator, P_1 and P_2 are the pressures inside the two chambers of the actuator, B is combined coefficient of the modeled damping and viscous friction forces, and y is the position output of the loading actuator caused by the movement of the aircraft actuator, f is the lumped uncertain nonlinearities due to external disturbances, the unmodeled friction forces and other hard-to-model terms.

The pressure dynamics can be written as [32]

$$\frac{V_t}{4\beta_e}\dot{P}_L = Q_L - C_t P_L - A\dot{y} \tag{2}$$

where V_{t} is the total control volume of the actuator; β_{e} is the effective oil bulk modulus; C_{t} is the coefficient of the total internal leakage of the actuator due to pressure; Q_{L} is the load flow.

In [2], although some researchers considered the dynamics of servo valve, the tracking performance improvement is not apparent. However, an additional sensor is required to measure the spool position and on the other hand, the design of controller becomes more complex, therefore the servo valve dynamics are not taken into consideration in many related works. Furthermore, provided the response performance of the servo valve is good enough, the spool displacement is directly proportional to the control input voltage, i.e., $x_{\mathrm{v}} = k_{\mathrm{i}}u$, where k_{i} is a positive constant, u is the control input voltage. So Q_{L} can be modeled by

$$Q_L = K_q x_v - K_c P_L \tag{3}$$

where K_{q} is the flow gain, K_{c} is the flow-pressure coefficient, x_{v} is the spool displacement.

Assumption 1: In general working conditions, according to the definition of P_1 and P_2, the system states of hydraulic system P_1 and P_2 are both bounded, i.e. $0 < P_{\mathrm{r}} < P_1 < P_{\mathrm{s}}$, $0 < P_{\mathrm{r}} < P_2 < P_{\mathrm{s}}$.

By observing Eqs. (1), (2) and (3), and defining the state variables $x_1 = T$, the dynamic model of EHLS can be rewritten by

$$\frac{V_t}{4A\beta_e g}\dot{x}_1 = u - \frac{K_t}{Ag}x_1 - \frac{K_t}{Ag}B\dot{y} - \frac{A}{g}\dot{y} - \frac{V_t B}{4A\beta_e g}\ddot{y} - d \tag{4}$$

where g$= k_{\mathrm{i}}K_{\mathrm{q}}$ is the total flow gain with respect to the control input u, K_{t} is the coefficient of the total leakage of the actuator about pressure, $d = \frac{K_t}{gA}f + \frac{V_t}{4A\beta_e g}\dot{f}$ represents all unmodelled uncertainties, which are assumed to be continuous differentiable functions of their respective variables.

For any force command, the following assumption is made.

Assumption 2: The desired force command $x_{1\mathrm{d}} = T_d(t)$ is third order continuous and differentiable. The displacement command $y_{\mathrm{d}}(t)$ and its fourth order continuous and differential. The motion disturbances $y, \dot{y}, \ddot{y}, \dddot{y}$ are also bounded.

III. NONLINEAR CONTROLLER DESIGN

A. DESIGN MODEL AND ISSUES TO BE ADDRESSED

To explicate the controller design procedure and simplify the controller implementation with respect to the unmodeled uncertainties, define the unknown but constant system parameter set $\theta = [\theta_1, \theta_2, \theta_3, \theta_4]^{\mathrm{T}}$, where $\theta_1 = V_t/(4A\beta_e g)$, $\theta_2 = K_t/(\mathrm{gA})$, $\theta_3 = K_t B/(gA) + A/g$, $\theta_4 = V_t B/(4A\beta_e g)$. Thus the equation (4) can be transformed into

$$\theta_1\dot{x}_1 = u - \theta_2 x_1 - \theta_3\dot{y} - \theta_4\ddot{y} - d(y, \dot{y}) \tag{5}$$

In equation (5), although $d(y, \dot{y})$ is unknown, it will present the periodicity after performing some cycles because the tracked trajectory y_{d} is period. Hence the repetitive control is taken into consideration to cope with the periodic-like disturbances $d(y, \dot{y})$. In addition, the parts multiplied with the system parameters are dependent on the actual states, which are normally contaminated with measurement noise. Based on this important observation, the equation (5) can be written as

$$\begin{aligned}\theta_1\dot{x}_1 = u - \theta_2 x_{1d} - \theta_3\dot{y}_d - \theta_4\ddot{y}_d - d(y_d, \dot{y}_d) \\ - \theta_2(x_1 - x_{1d}) + \Delta\end{aligned} \tag{6}$$

where Δ represents approximation errors defined by

$$\Delta = -\theta_3(\dot{y} - \dot{y}_d) - \theta_4(\ddot{y} - \ddot{y}_d) - [d(y, \dot{y}) - d(y_d, \dot{y}_d)] \tag{7}$$

In (7), $d(y_d, \dot{y}_d)$ is the desired version of $d(y, \dot{y})$. For simplicity, $d(y_d, \dot{y}_d)$ is represented by $D_{\mathrm{d}}(t)$ in the following controller design.

Many hydraulic servomechanisms are required to deal with repetitive tasks in practice, for example, hydraulic actuator, manipulators and testing equipments are often asked to perform the same motion over and over again. Hence, for these applications, the desired signal $x_{1\mathrm{d}}$ is periodic. Namely,

$$x_{1d}(t - T) = x_{1d}(t) \tag{8}$$

where T is the known period.

It is easy to know $\dot{x}_{1d}$ is also periodic. Since D_{d} is only the functions of $x_{1\mathrm{d}}$ and $\dot{x}_{1d}$, it is clear that the unknown nonlinear functions $D_{\mathrm{d}}(\mathrm{t})$ is also periodic, i.e.,

$$D_d(t-T) = D_d(t) \tag{9}$$

According to Fourier series, the unknown periodic nonlinear functions $D_{\mathrm{d}}(t)$ can be written as

$$D_d(t) = \frac{A_0}{2} + \sum_{n=1}^{m} (A_n \cos n\omega t + B_n \sin n\omega t), \quad m < \infty \tag{10}$$

In order to simplify the system equation, define the unknown but constant parameter set $\psi = [A_0/2, A_1, B_1, \ldots, A_{\mathrm{m}}, B_{\mathrm{m}}]^{\mathrm{T}}$. Thus, with equation (10), we can transfer the system model (6) into

$$\theta_1 \dot{x}_1 = u - \theta_2 x_{1d} - \theta_3 \dot{y}_d - \theta_4 \ddot{y}_d - \phi^T \psi - \theta_2 (x_1 - x_{1d}) + \Delta \tag{11}$$

where $\phi = [1, \cos\omega t, \sin\omega t, \cdots, \cos m\omega t, \sin m\omega t]^T$.

Although the true values of the unknown parameter set θ and ψ are not known, the range of the parametric uncertainties and uncertain nonlinearities are known for most applications. Thus the following practical assumption is made.

Assumption 3:

$$\begin{cases} \theta \in \Omega_\theta = \{\theta : \theta_{\min} \le \theta \le \theta_{\max}\} \\ \psi \in \Omega_\psi = \{\psi : \psi_{\min} \le \psi \le \psi_{\max}\} \\ \left|\dot{\Delta}(t)\right| \le \delta_1, \left|\ddot{\Delta}(t)\right| \le \delta_2 \end{cases} \tag{12}$$

where $\theta_{\min} = [\theta_{1\min}, \ldots, \theta_{4\min}]^{\mathrm{T}}$, $\theta_{\max} = [\theta_{1\max}, \ldots, \theta_{4\max}]^{\mathrm{T}}$, $\psi_{\min} = [\psi_{1\min}, \ldots, \psi_{5\min}]^{\mathrm{T}}$, $\psi_{\max} = [\psi_{1\max}, \ldots, \psi_{5\max}]^{\mathrm{T}}$ and δ_1, δ_2 are known constants.

B. CONTROLLER DESIGN

A set of quantities are defined as

$$z_1 = x_1 - x_{1d}, \quad r = \dot{z}_1 + k_1 z_1 \tag{13}$$

where k_1 is a positive feedback gain, $r(t)$ is an auxiliary error signal defined to get an extra design freedom. It is noticeable that the filtered tracking error $r(t)$ cannot be measured because it depends on the time derivative of force sample, moreover, its main function is just to help the following controller design. From (13), represent the formula of r as

$$\theta_1 r = \theta_1 \dot{x}_1 - \theta_1 \dot{x}_{1d} + \theta_1 k_1 z_1 \tag{14}$$

Based on the system model (11), we now have

$$\theta_1 r = u - \theta_2 x_{1d} - \theta_3 \dot{y}_d - \theta_4 \ddot{y}_d - \phi^T \psi + \Delta - \theta_2 z_1 + \theta_1 k_1 z_1 - \theta_1 \dot{x}_{1d} \tag{15}$$

Thus the resulting model-based controller can be considered by

$$\begin{aligned} u &= u_a + u_s, u_s = u_{s1} + u_{s2} \\ u_a &= \hat{\theta}_1 \dot{x}_{1d} + \hat{\theta}_2 x_{1d} + \hat{\theta}_3 \dot{y}_d + \hat{\theta}_4 \ddot{y}_d + \phi^T \hat{\psi} \\ u_{s1} &= -k_r z_1, u_{s2} = -\int_0^t k_1 k_r z_1 + \beta \mathrm{sgn}(z_1) dv \\ \dot{\hat{\theta}} &= -\Gamma_\theta \dot{\varphi} r, \dot{\hat{\psi}} = -\Gamma_\psi \dot{\phi} r \end{aligned} \tag{16}$$

where u_a is a mode-based feed-forward compensation term which can be adjusted by parameter adaptation, u_{s} is a robust control term to cope with the time-variant disturbance $\Delta(t)$, $\hat{\theta}$ denotes the estimate of θ and $\tilde{\theta}$ the estimation error (i.e., $\tilde{\theta} = \hat{\theta} - \theta$), $\hat{\psi}$ denote the estimate of ψ and $\tilde{\psi}$ the estimation error (i.e., $\tilde{\psi} = \hat{\psi} - \psi$), k_{r} is a positive feedback gain, $\Gamma_\theta, \Gamma_\psi > 0$ are diagonal adaptation rate matrix, $\varphi = [\dot{x}_{1d}, x_{1d}, \dot{y}_d, \ddot{y}_d]^T$ is a regressor and sgn(*) is defined as

$$sgn(^*) = \begin{cases} 1, & \text{if } ^* \ge 0 \\ 0, & \text{if } ^* < 0 \end{cases} \tag{17}$$

According to the parameter adaptation law in (16), it is noticeable that although the signal $r(t)$ is unknown, the vectors $\dot{\phi}, \dot{\varphi}$ and their time derivative are known because they are based on the trajectory, therefore, the parameter adaptation laws for θ and ψ can be synthesized as follows

$$\begin{aligned} \hat{\theta}(t) &= \hat{\theta}(0) - \Gamma_\theta \dot{\varphi} z_1 + \Gamma_\theta \int_0^t \ddot{\varphi} z_1 dv - \Gamma_\theta \int_0^t k_1 \dot{\varphi} z_1 dv \\ \hat{\psi}(t) &= \hat{\psi}(0) - \Gamma_\psi \dot{\phi} z_1 + \Gamma_\psi \int_0^t \ddot{\phi} z_1 dv - \Gamma_\psi \int_0^t k_1 \dot{\phi} z_1 dv \end{aligned} \tag{18}$$

Some advantages of the developed controller are listed below: (i) This controller can apparently reduce the effect of measurement noise because the system states related to the control input only rely on the desired trajectory. (ii)The computation time and occupation memory can be greatly saved because ϕ and φ and their time derivative can be computed offline. (iii) The process of gain tuning becomes simpler because u_a and u_{s} are independent. (iiii) The synthesized controller is continuous, which is much more applicable in practical applications.

Substituting (16) into (15), we can obtain

$$\theta_1 r = \tilde{\theta}^T \varphi + \tilde{\psi}^T \phi + \Delta - k_r z_1 - k_2 z_1 + u_{s2} \tag{19}$$

where $k_2 = \theta_2 - \theta_1 k_1$ and the time derivative of (19) can be given by

$$\theta_1 \dot{r} = \dot{\tilde{\theta}}^T \varphi + \tilde{\theta}^T \dot{\varphi} + \dot{\tilde{\psi}}^T \phi + \tilde{\psi}^T \dot{\phi} + \dot{\Delta} - k_r r - k_2 (r - k_1 z_1) - \beta \mathrm{sgn}(z_1) \tag{20}$$

C. MAIN RESULTS

Before stating the main results, the following lemma is introduced and will be cited later.

Lemma 1: An auxiliary function $L(t)$ is defined as

$$L(t) = r\left[\dot{\Delta}(t) - \beta \text{sgn}(z_1)\right] \tag{21}$$

Provided the gain β is chosen to satisfy the following inequation:

$$\beta \geq \delta_1 + \frac{1}{k_1}\delta_2 \tag{22}$$

Thus the function $P(t)$ defined below is always positive,

$$P(t) = \beta |z_1(0)| - z_1(0)\dot{\Delta}(0) - \int_0^t L(v)dv \tag{23}$$

Proof: See Appendix A.

Theorem 1: According to the adaptation law (18), the following defined matrix Λ is positive definite by choosing the gain β satisfying inequality (22) and feedback gains k_1, k_2, k_3 and k_r large enough

$$\Lambda = \begin{Bmatrix} k_1 & -\frac{k_1k_2+1}{2} \\ -\frac{k_1k_2+1}{2} & k_3 \end{Bmatrix} \tag{24}$$

where $k_3 = \lfloor k_2 + k_r - \max\{|\dot{\varphi}^T\Gamma_\theta\varphi|\} - \max\{|\dot{\phi}^T\Gamma_\psi\phi|\}\rfloor$ in which $\max\{\cdot\}$ denotes the maximum value of matrix $\cdot$, thus the proposed control law (16) guarantees that all system signals are bounded under closed-loop circumstance, and asymptotic output tracking is also achieved, i.e., $z_1 \to 0$ as $t \to \infty$.

Proof: See Appendix B.

Remark 1: Consequences of **Theorem1** demonstrate that the developed controller has an adjustable asymptotic tracking capability, which is vital for the high-accuracy tracking control of hydraulic systems, however, the unknown uncertainties are still the main difficulties for high-accuracy tracking, especially when performing periodic tasks. Besides, although it seems that assumption 3 presents a strong restriction on the lumped uncertain nonlinearities, which may weaken the results in **Theorem 1**, actually this practical assumption will be satisfied for certain sets of $\delta_1(t)$ and $\delta_2(t)$, at least locally around the desired trajectory to be tracked.

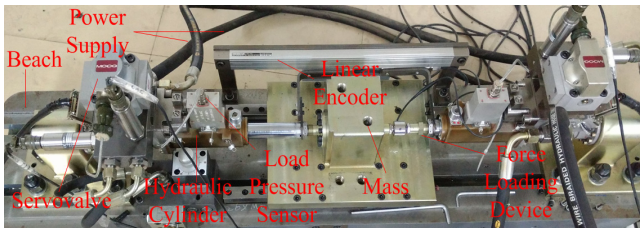

FIGURE 2. Experimental equipment of hydraulic actuator.

IV. COMPARATIVE EXPERIMENTAL RESULTS

A. EXPERIMENT SETUP

The effectiveness and feasibility of the proposed control approach for the electro-hydraulic load simulator was validated on a hydraulic actuator platform. As is illustrated in Fig. 2, this platform is made up of a bench case, an EHLS, an encoder, two pressure sensors, a high bandwidth servo valve, a shaft joint and a motion actuator. In addition, there are a set of inertial steel sheets, a hydraulic supplier, a measurement and control software. Specifications of hardware components are listed in Table 1. The measurement and control software include a monitor software and a real time control software. The monitor software is programmed with NI LabWindows/CVI, and the real time control software is compiled with Microsoft visual studio 2005 plus Ardence RTX 7.0, which is utilized to offer a real-time environment for real time control software under Windows XP operating system. And the sampling time T is 0.5 ms.

TABLE 1. Specifications of the EHLS and aircraft actuation system.

Components	Specifications	
Hydraulic supply	Supply pressure	120 bar
Servo valve	Type	Moog G761-3003
	Rated flow	19L/min at 70 bar drop
	Bandwidth	≥120 Hz
Hydraulic actuator	Stroke	44mm
	Efficient ram area	904.78 mm2
Load mass	Mass	30 kg
Linear encoder	Type	Heidenhain LC483
	Accuracy	±5 μm
Pressure sensors	Type	MEAS US175-C00002-200BG
	Accuracy	1 bar
A/D card	Type	Advantech PCI-1716
D/A card	Type	Advantech PCI-1723
Counter card	Type	Heidenhain IK-220
Computer	Type	IEI WS-855GS

B. COMPARATIVE RESULTS

In order to validate the effectiveness and feasibility of the proposed control approach, the following four controllers are compared.

1) APRISE: This is the proposed adaptive repetitive controller with RISE feedback developed in this paper and described in Section III. As in [2], for simplicity, the feedback gains k_1, k_r, β are chosen large enough so that the system stability can be guaranteed. Thus, the following control gains are utilized: $k_1 = 1$, $k_r = 3.2 \times 10^{-4}$, $\beta = 0.01$. In order to prove that the parameters can converge to a correct value under parameter adaptation law, all estimates of θ begin at zero. Meanwhile, the robustness of the ARISE controller is also proved even under the circumstance of large parameters error. The parameter adaptation rates are set at $\Gamma_\theta = \text{diag}\{5 \times 10^{-15}, 2 \times 10^{-10}, 1 \times 10^{-2}, 1 \times 10^{-5}\}$, $1\ \Gamma_\psi = \text{diag}\{0, 1 \times 10^{-4}, 1 \times 10^{-4}, 1 \times 10^{-4}, 1 \times 10^{-4}\}$. When adjusting the parameters, it is

noticeable that the feedback gains should be adjusted first. After that, when adjusting θ and ψ, the feedback gains just need to be adjusted slightly around the values determined before.

2) ARC: This is the adaptive robust controller developed in [5], [14], and [15]. However, the results in [5] cannot be utilized directly since the formulated system models are different. To apply the ARC method to our EHLS, the system dynamic model is formulated as

$$\vartheta_1\dot{x}_1 = u - \vartheta_2 x_{1d} - \vartheta_3\dot{y}_d - \vartheta_4\ddot{y}_d - \vartheta_2(x_1 - x_{1d}) + \tilde{\Delta} \tag{25}$$

where $\vartheta_1 = V_t/(4A\beta_e g)$, $\vartheta_2 = K_t/(gA)$, $\vartheta_3 = K_t B/(gA) + A/g$, $\vartheta_4 = V_t B/(4A\beta_e g)$ represent the unknown but constant parameters which will be adapted in ARC, $\tilde{\Delta} = -\theta_3(\dot{y}-\dot{y}_d) - \theta_4(\ddot{y}-\ddot{y}_d) - d(y,\dot{y})$ denotes the unmodeled disturbances. Define a parameter set as $\vartheta = [\vartheta_1, \vartheta_2, \vartheta_3, \vartheta_4]^{\mathrm{T}}$ and let $\hat{\vartheta}$ represent the online estimation of ϑ, which is adapted by $\dot{\hat{\vartheta}} = \mathrm{Pr}oj(\Gamma_\vartheta \tau)$, where $\Gamma_\vartheta > 0$ is a diagonal adaptation rate matrix, τ is an adaptation function to be summarized later. Following the design procedure in [5], [14], and [15], the ARC controller can be synthesized as

$$u = \hat{\theta}_1\dot{x}_{1d} + \hat{\theta}_2 x_{1d} + \hat{\theta}_3\dot{y}_d + \hat{\theta}_4\ddot{y}_d - k_1 z_1 - \frac{h}{4\varepsilon}z_1 \tag{26}$$

where h be any smooth function satisfying $h \geq \|\vartheta_M\|^2 \|\varphi_\vartheta\|^2 + \delta_d^2$, $\vartheta_{\mathrm{M}} = \vartheta_{\max} - \vartheta_{\min}$, $\varepsilon > 0$ is a parameter to be designed.

The parameter adaptation function $\tau = -\phi_\vartheta z_1$, where $\varphi_\vartheta = [\dot{x}_{1d}, x_{1d}, \dot{y}_d, \ddot{y}_d]^T$.

The ARC controller parameters are chosen as: $k_1 = 1$; the bounds of ϑ are given as: $\vartheta_{\min} = [0, 0, 10, 0]^{\mathrm{T}}$; $\vartheta_{\max} = [2\times10^{-6}, 4\times10^{-5}, 52, 0.01]^{\mathrm{T}}$. The adaptation rates are set at $\Gamma_\vartheta = \mathrm{diag}\{5\times10^{-15}, 2\times10^{-10}, 1\times10^{-2}, 1\times10^{-5}\}$.

3) FLC: This is the feedback linearization controller (FLC). The only difference between FLC and ARC is that the former has no parameter adaptation. All system parameters in this method start at their initial values, i.e., $\hat{\vartheta}(t) = \hat{\vartheta}(0)$ with $\Gamma_\vartheta = 0$ to prove the effectiveness and feasibility of the parameter estimation method developed in this paper. Other controller parameters in FLC and ARC are correspondingly identical.

4)VPID: This is the proportional-integral-derivative controller based on velocity synchronizing-compensation method by using the control signal of the control actuator, which is widely utilized in industries and can reduce the lagging effects for the better performance [2]. The controller gains are tuned as $k_{\mathrm{p}} = 0.1$, $k_{\mathrm{i}} = 0.05$, $k_{\mathrm{d}} = 0$, which represent the P-gain, I-gain, and D-gain respectively. The synchronization coefficient of this controller is 1. The overall scheme of VPID is illustrated in Fig. 3, in which θ_{r} and θ_{f} is the displacement command and output of actuator respectively, M_{r} and M_{f} is the force command and output of EHLS respectively.

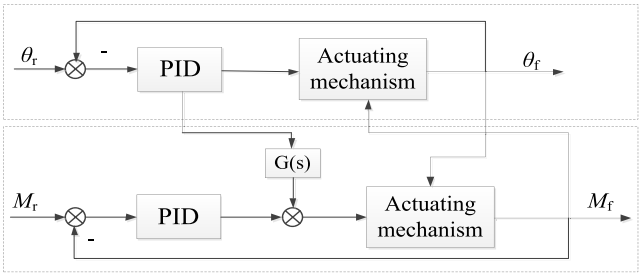

FIGURE 3. The velocity synchronizing control scheme.

Besides, three performance indexes will be calculated to access the quality of each controller as follows, i.e., the maximum, average, and standard deviation of the tracking errors. The definitions of the three indexes are given below

1) Maximal absolute value of the tracking errors is defined as

$$M_e = \max_{i=1,\ldots,N}\{|z_1(i)|\} \tag{27}$$

where N is the number of the recorded digital signals, and is used as an index of measure of tracking accuracy.

2) Average tracking error is defined as

$$\mu = \frac{1}{N}\sum_{i=1}^{N}|z_1(i)| \tag{28}$$

and is used as an objective numerical measure of average tracking performance.

3) Standard deviation performance index is defined as

$$\sigma = \sqrt{\frac{1}{N}\sum_{i=1}^{N}[|z_1(i)| - \mu]^2} \tag{29}$$

to measure the deviation level of tracking errors.

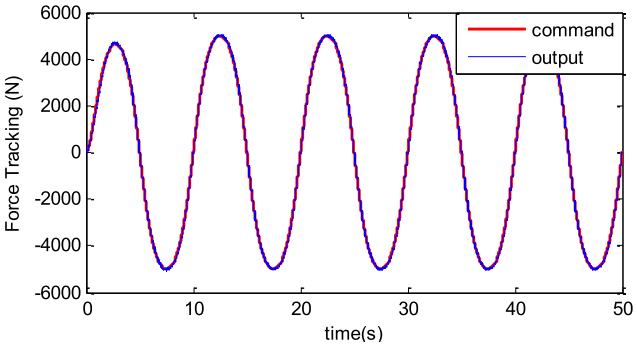

FIGURE 4. Tracking performance of APRISE for 0.1 Hz.

To test the tracking capability of the proposed approach, the experimental command is set as a sinusoidal-like periodic trajectory. The desired force trajectory is $T_{\mathrm{d}} = 5000\sin(0.314t)[1 - \exp(-0.5t^3)]$ N and is shown in Fig. 4.

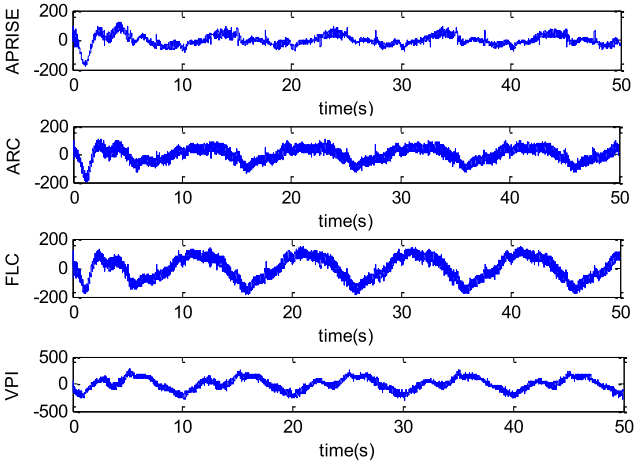

FIGURE 5. Tracking errors of the four controllers for 0.1 Hz.

TABLE 2. Performance indexes for 0.1 HZ.

Indexes	M_e	μ	σ
APRISE	89.5651	23.9958	17.8429
ARC	131.0170	39.7438	23.4121
FLC	182.8250	71.5918	36.5578
VPID	302.0832	91.3063	61.6254

The motion disturbance from the aircraft actuator is given by $y = 0.02\sin(0.314t)[1 - \exp(-0.5t^3)]$ m. Fig.5 demonstrates the tracking precision of the four controllers. And Table 2 demonstrates the performance indexes during the last three cycles to explore the final tracking performance, which is pretty significant for hydraulic system to perform repetitive work. According to these experimental results, it is obvious that the proposed APRISE controller achieved the most excellent tracking performance in comparison to other three controllers among all performance indexes. The tracking error of APRISE converges to a small level after the starting period, which verifies the proposed nonlinear force controller. This verifies the effectiveness of the proposed scheme with appropriate model-based adaptive repetitive law, which can effectively compensate the periodic-like uncertainties in EHLS. However, although the parameter adaptation law is utilized in ARC controller, its ability to deal with the hard-to-model terms is inferior to APRISE, especially encountering those related to the system states. Therefore, these unmodeled uncertainties and disturbances can heavily deteriorate the tracking performance of traditional adaptive controllers. However, although the nonlinear friction is not considered in the model, it is clear that the unmodelling uncertainties and disturbances in EHLS can be restrained by the proposed RISE feedback term validly, resulting in an improved tracking performance achieved by APRISE. The tracking performance of the simple model-based FLC

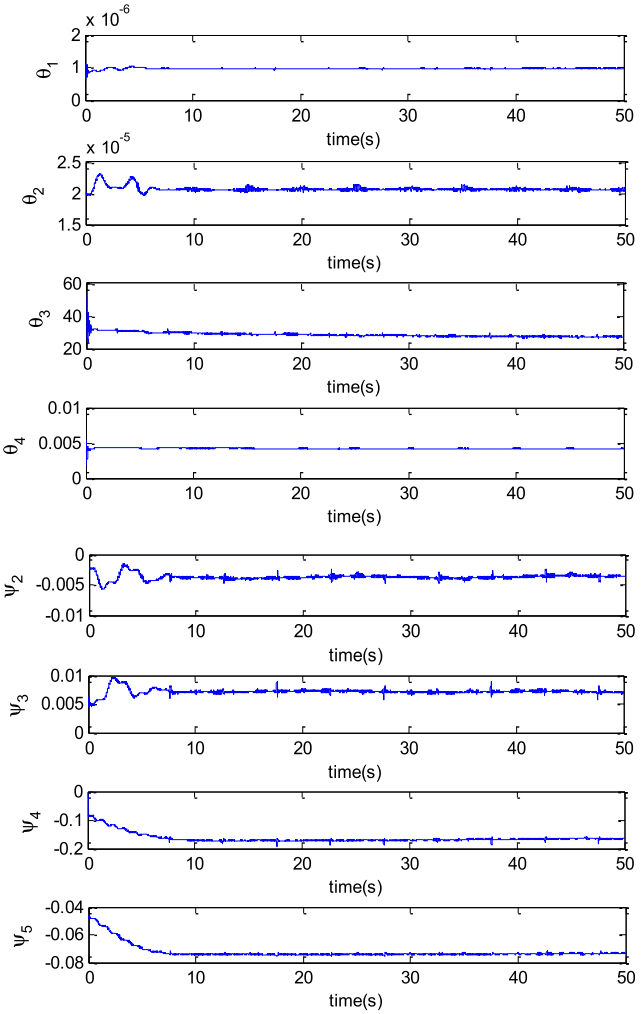

FIGURE 6. Parameter estimation of APRISE for 0.1 Hz.

controller is inferior to ARC controller but superior to VPID controller which only employed the robustness against the uncertainties and disturbances, demonstrating the effectiveness of parameter adaption and the benefits of the model-based controller design method.

Besides, as seen from Table 2, compared with the other three controllers, the standard deviation of the tracking errors of APRISE is the least, which means the chattering is also the least under APRISE controller. It is because the regressor functions φ and ϕ in APRISE controller are all dependent on desired functions which will not be influenced by the noise pollution, and consequently, the parameter adaptation and adjustable compensation parts are less noise sensitivity.

Furthermore, In order to prove the effectiveness of parameter estimations, the initial parameter estimations are set far away from their optimal values manually and deliberately. And due to the poor initial parameter estimations, the transient performance of APRISE is not good. However, as shown in Fig. 5, after the beginning period, the designed adaptation law can achieve excellent final tracking performance. From Fig. 6 and Fig. 7, the convergence performance of

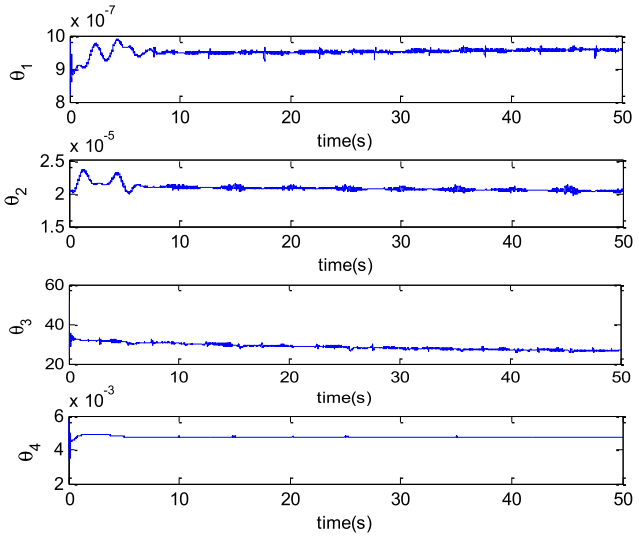

FIGURE 7. Parameter estimation of ARC for 0.1 Hz.

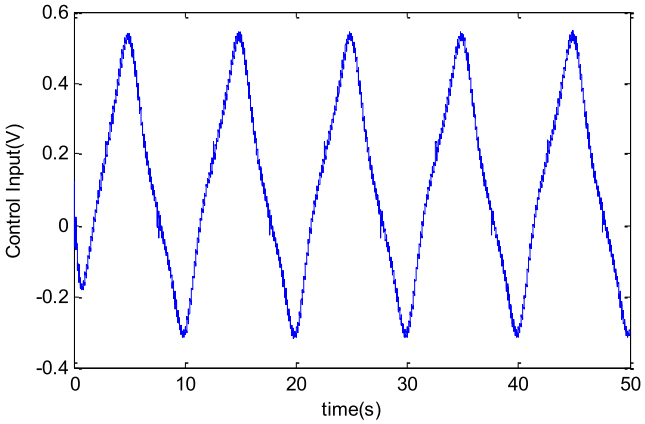

FIGURE 8. Control input of APRISE for 0.1 Hz.

the parameter estimation of ARISE is satisfying, namely the effectiveness of the parameter adaption method is verified. From the expression of ϕ and adaption law (18), we can know that ψ_1 is always equal to its initial value, thus the parameter estimation of ψ_1 is not presented in Fig. 6. Fig. 8 illustrates the control input of the proposed APRISE controller, which is continuous and bounded.

It is noticeable that in practical industrial implementations, the poor transient performance may be not acceptable. Therefore, to enhance the transient tracking capability, it is suggested to use a set of possible off-line estimated parameters to initialize the controller.

To further investigate the tracking capability of the proposed controller with respect to rapid varying uncertainties, experiments are run for a fast motion sinusoidal-like periodic trajectory. The desired force command is set by $T_\mathrm{d} = 10000\sin(1.57t)[1 - \exp(-0.5t^3)]$ N and the motion disturbance is set by $y = 0.02\sin(1.57t)[1 - \exp(-0.5t^3)]$ m. Fig. 9 illustrates the tracking performance of the four controllers and Table 3 presents the

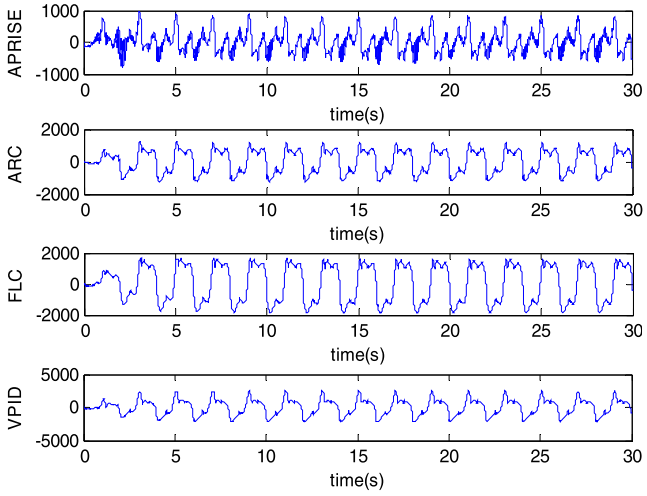

FIGURE 9. Tracking errors of the four controllers for 0.5 Hz.

TABLE 3. Performance indexes for 0.5 HZ.

Indexes	M_e	μ	σ
APRISE	831.6956	263.8449	193.0312
ARC	1209.3012	687.0937	258.0407
FLC	1896.9173	1221.3482	372.8117
VPID	2484.5906	1110.1214	589.7579

corresponding performance indexes during the last five cycles. In this experimental part, the tracking capability is mainly influenced by those unmodeled rapid-varying disturbance, which can be utilized to validate the learning ability of the designed APRISE controller. According to these test results, it is obvious that the synthesized APRISE algorithm is superior to the other three controllers even under such a challenging tracking circumstance. Comparing with ARISE, the tracking performance of ARC is worse because it cannot alleviate the unknown disturbance effectively, especially in high frequency situation.

Since the tracking performance of FLC is largely dependent on the initial values of the parameters, the fact FLC is better than VPID shows that the initial values of FLC are reasonable. However, the performance difference between FLC and VPID is getting smaller compared with the situation of 0.1 Hz, the reason is that with the frequency increasing, the model-based control term cannot gradually compensate the model very well. Without parameter adaption, the parameter deviation between the initial values and real values will enlarge the tracking error of the model-based control when the tracking frequency increases.

To the end, a rapid desired force command $T_\mathrm{d} = 10000\sin(3.14t)[1 - \exp(-0.5t^3)]$ N and the motion disturbance $y = 0.02\sin(3.14t)[1 - \exp(-0.5t^3)]$ m are given to verify the tracking performance in this aggressive test. Under this condition, the tracking performance of the

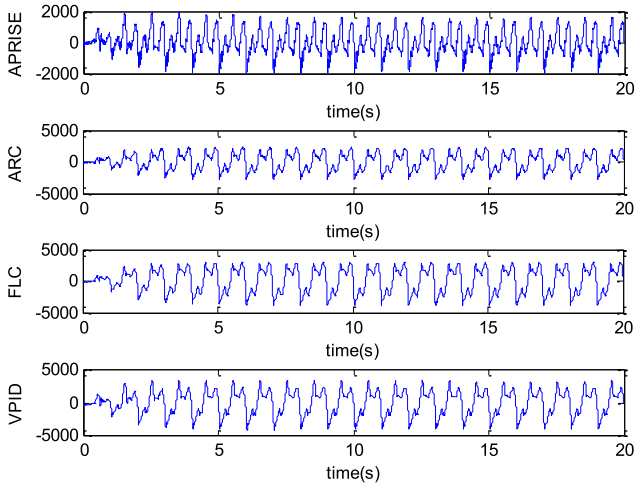

FIGURE 10. Tracking errors of the four controllers for 1 Hz.

TABLE 4. Performance indexes for 1 HZ.

Indexes	M_e	μ	σ
APRISE	1922.5199	655.4376	461.2756
ARC	2776.0711	1258.6628	637.4321
FLC	3866.1554	1920.4445	799.5979
VPID	4163.3636	1749.8099	903.3906

four controllers are shown in Fig. 10 and corresponding performance indexes during the last ten cycles are collected in Table 4. As seen, though the motion disturbance has tremendously increased, the proposed APRISE controller is able to attenuate unexpected effects and holds the tracking accuracy in a satisfactory level, while other three controllers are unable to complete this challenging task satisfactorily. The tracking performance of traditional ARC controller has been heavily deteriorated by the hard-to-model terms (i.e., unmodeled disturbances and uncertainties) under such a challenging condition. In addition, it is noticeable that the performance of FLC is decreasing and be close to VPID, which verifies the importance of parameters adaption again.

V. CONCLUSION

This paper synthesized an adaptive repetitive controller with RISE robust feedback throughout a Fourier series approximation for EHLS. To cope with the parametric uncertainties and unmodeled disturbances, an adjustable model-based controller is then synthesized by employing the smoothness of the considered disturbances and their priori bounds. In this novel control scheme, a nonlinear robust feedback term contains the integral of the sign of the error and parameter adaptations are integrated. The developed controller can obtain the excellent asymptotic tracking result, which can be theoretically verified by Lyapunov analysis. Besides, extensive experiment results are also obtained for an EHLS test equipment to validate the high-performance characteristic of the proposed scheme.

APPENDIX A

Proof of Lemma 1: After substituting the definition of r in (13) into (21), and by integrating in time, we have

$$\begin{aligned}\int_0^t L(v)dv &= \int_0^t (\dot{z}_1 + k_1 z_1)\left[\dot{\Delta} - \beta \mathrm{sgn}(z_1)\right]dv \\ &= \int_0^t \dot{z}_1 \dot{\Delta} dv - \int_0^t \dot{z}_1 \beta \mathrm{sgn}(z_1) dv \\ &\quad + \int_0^t k_1 z_1 \left[\dot{\Delta} - \beta \mathrm{sgn}(z_1)\right]dv \end{aligned} \tag{A1}$$

And then based on integration by parts, the first integral on the right-hand side in (A1) can be dealt with, now we have

$$\begin{aligned}\int_0^t L(v)dv &= z_1 \dot{\Delta}\big|_0^t - \int_0^t z_1 \ddot{\Delta} dv - \beta |z_1|_0^t \\ &\quad + \int_0^t k_1 z_1 \left[\dot{\Delta} - \beta sgn(z_1)\right] dv \\ &= z_1 \dot{\Delta} - z_1(0)\dot{\Delta}(0) - \beta |z_1| + \beta |z_1(0)| \\ &\quad + \int_0^t k_1 \left[z_1 \dot{\Delta} - \frac{1}{k_1} z_1 \ddot{\Delta} - \beta |z_1|\right] dv \end{aligned} \tag{A2}$$

The upper bound of the right-hand side in (A2) can be described as follows:

$$\begin{aligned}\int_0^t L(v)dv &\le |z_1| \left|\dot{\Delta}\right| - z_1(0)\dot{\Delta}(0) - \beta |z_1| \\ &\quad + \beta |z_1(0)| + \int_0^t k_1 |z_1| \left[\left|\dot{\Delta}\right| + \frac{|\ddot{\Delta}|}{k_1} - \beta\right] dv \end{aligned} \tag{A3}$$

From condition (12), it is known from (A3) that if β satisfies (22), then the function $P(t)$ defined in (23) is always positive, so the lemma 1 is proved.

APPENDIX B

Proof of Theorem 1: Defining a Lyapunov function as

$$V = \frac{1}{2}z_1^2 + \frac{1}{2}\theta_1 r^2 + \frac{1}{2}\tilde{\theta}^T \Gamma_\theta^{-1} \tilde{\theta} + \frac{1}{2}\tilde{\psi}^T \Gamma_\psi^{-1} \tilde{\psi} + P(t) \tag{B1}$$

It is easy to know V is positive. Based on (13), (16) and (20), its time derivative of V is

$$\begin{aligned}\dot{V} &= z_1(r - k_1 z_1) + \dot{\hat{\theta}}^T \varphi r + \tilde{\theta}^T \dot{\varphi} r + \dot{\hat{\psi}}^T \phi r + \tilde{\psi}^T \dot{\phi} r \\ &\quad - k_r r^2 - k_2 r^2 + k_1 k_2 z_1 r + r\left[\dot{\Delta} - \beta sgn(z_1)\right] + \dot{P}(t) \end{aligned} \tag{B2}$$

Noting the adaptive law (18), we have

$$\begin{aligned} V &= k_1 z_1^2 + z_1 r - (k_2 + k_r) r^2 + k_1 k_2 z_1 r \\ &\quad - \dot{\varphi}^T \Gamma_\theta \varphi r^2 - \dot{\phi} \Gamma_\psi \phi r^2 \\ &\le -k_1 z_1^2 + (k_1 k_2 + 1) z_1 r \\ &\quad - \left[k_2 + k_r - \max\left\{\dot{\varphi}^T \Gamma_\theta \varphi r^2\right\} - \max\left\{\dot{\phi} \Gamma_\psi \phi r^2\right\}\right] r^2 \\ &\le -k_1 z_1^2 + (k_1 k_2 + 1) z_1 r - k_3 r^2 \end{aligned} \tag{B3}$$

Note that the matrix Λ defined in (24) is positive definite, we can upper bound the above equation as

$$\dot{V} \leq -z^T \Lambda z \leq -\lambda_{\min}(\Lambda)(z_1^2 + r^2) = -W \qquad \text{(B4)}$$

where z is defined by $z = [z_1, r]^{\mathrm{T}}$, $\lambda_{\min}(\Lambda)$ represents the minimal eigenvalue of matrix Λ. Thus, $V \in L_\infty$ and $W \in L_2$, the signal$z$ and the parameter estimation are bounded, which means that x_1 is bounded. Hence the control input u is also bounded. According to the dynamics of z_1 and r, the time derivative of W can be inferred to be bounded, thus W is uniformly continuous. On the basis of Barbalat's lemma, $W \to 0$ as $t \to \infty$, and the conclusions in **Theorem 1** are proved.

REFERENCES

[1] J. Yao, Z. Jiao, and D. Ma, "High dynamic adaptive robust control of load emulator with output feedback signal," *J. Franklin Inst.*, vol. 351, no. 8, pp. 4415–4433, 2014.

[2] Z.-X. Jiao, J.-X. Gao, Q. Hua, and S.-P. Wang, "The velocity synchronizing control on the electro-hydraulic load simulator," *Chin. J. Aeronaut.*, vol. 17, no. 1, pp. 39–46, 2004.

[3] B. Yang, R. Bao, and H. Han, "Robust hybrid control based on PD and novel CMAC with improved architecture and learning scheme for electric load simulator," *IEEE Trans. Ind. Electron.*, vol. 61, no. 10, pp. 5271–5279, Oct. 2014.

[4] J. Zhao, G. Shen, W. Zhu, C. Yang, and J. Yao, "Robust force control with a feed-forward inverse model controller for electro-hydraulic control loading systems of flight simulators," *Mechatronics*, vol. 38, pp. 42–53, Sep. 2016.

[5] J. Yao, Z. Jiao, B. Yao, Y. Shang, and W. Dong, "Nonlinear adaptive robust force control of hydraulic load simulator," *Chin. J. Aeronaut.*, vol. 25, no. 5, pp. 766–775, 2012.

[6] D. Q. Truong and K. K. Ahn, "Force control for hydraulic load simulator using self-turning grey predictor—Fuzzy PID," *Mechatronics*, vol. 19, no. 2, pp. 233–246, 2009.

[7] K. K. Ahn and H. T. C. Nguyen, "Force control of hybrid actuator using learning vector quantization neural network," *J. Mech. Sci. Technol.*, vol. 20, no. 4, pp. 447–454, 2006.

[8] S. Hara, Y. Yamamoto, T. Omata, and M. Nakano, "Repetitive control system: A new type servo system for periodic exogenous signals," *IEEE Trans. Autom. Control*, vol. 33, no. 7, pp. 659–668, Jul. 1988.

[9] T. Wang and Z. Zhou, "A compact hydrostatic-driven electric generator: Design, prototype, and experiment," *IEEE/ASME Trans. Mechatronics*, vol. 21, no. 3, pp. 1612–1619, Jun. 2016.

[10] B. Yao and L. Xu, "On the design of adaptive robust repetitive controllers," in *Proc. ASME Int. Mech. Eng. Congr. Expo.*, vol. 4. 2001, pp. 1–9.

[11] P. Mercorelli and N. Werner, "A model of a servo piezo mechanical hydraulic actuator and its regulation using repetitive control," in *Proc. IEEE/ASME Int. Conf. Adv. Intell. Mechatronics*, 2014, pp. 186–191.

[12] C. Kempf, W. Messner, M. Tomizuka, and R. Horowitz, "Comparison of four discrete-time repetitive control algorithms," *IEEE Control Syst.*, vol. 13, no. 6, pp. 48–54, Dec. 1993.

[13] Q.-C. Zhong, W.-L. Ming, X. Cao, and M. Krstic, "Control of ripple eliminators to improve the power quality of DC systems and reduce the usage of electrolytic capacitors," *IEEE Access*, vol. 4, pp. 2177–2187, 2016.

[14] B. Yao and M. Tomizuka, "Adaptive robust control of SISO nonlinear systems in a semi-strict feedback form," *Automatica*, vol. 33, no. 5, pp. 893–900, May 1997.

[15] B. Yao, "High performance adaptive robust control of nonlinear systems: A general framework and new schemes," in *Proc. 36th IEEE Conf. Decision Control*, vol. 3. Dec. 1997, pp. 2489–2494.

[16] Z. Chen, B. Yao, and Q. Wang, "μ-synthesis-based adaptive robust control of linear motor driven stages with high-frequency dynamics: A case study," *IEEE/ASME Trans. Mechatronics*, vol. 20, no. 3, pp. 1482–1490, Jun. 2015.

[17] B. Yao and M. Tomizuka, "Smooth robust adaptive sliding mode control of manipulators with guaranteed transient performance," *ASME Trans. Dyn. Syst., Meas. Control*, vol. 118, no. 4, pp. 764–775, 1996.

[18] B. Yao and M. Tomizuka, "Adaptive robust control of MIMO nonlinear systems in semi-strict feedback forms," *Automatica*, vol. 37, no. 9, pp. 1305–1321, 2001.

[19] B. Yao, F. Bu, J. Reedy, and G. T. C. Chiu, "Adaptive robust motion control of single-rod hydraulic actuators: Theory and experiments," *IEEE/ASME Trans. Mechatronics*, vol. 5, no. 1, pp. 79–91, Mar. 2000.

[20] Z. Chen, Y.-J. Pan, and J. Gu, "Integrated adaptive robust control for multilateral teleoperation systems under arbitrary time delays," *Int. J. Robust Nonlinear Control*, vol. 26, no. 12, pp. 2708–2728, 2016.

[21] J. Yao, Z. Jiao, and D. Ma, "A practical nonlinear adaptive control of hydraulic servomechanisms with periodic-like disturbances," *IEEE/ASME Trans. Mechatronics*, vol. 20, no. 6, pp. 2752–2760, Dec. 2015.

[22] B. Yao, M. Al-Majed, and M. Tomizuka, "High performance robust motion control of machine tools: An adaptive robust control approach and comparative experiments," *IEEE/ASME Trans. Mechatronics*, vol. 2, no. 2, pp. 63–76, Jun. 1997.

[23] W. Sun, H. Gao, and O. Kaynak, "Finite frequency H_∞ control for vehicle active suspension systems," *IEEE Trans. Control Syst. Technol.*, vol. 19, no. 2, pp. 416–422, Mar. 2011.

[24] B. Xian, D. M. Dawson, M. S. D. Queiroz, and J. Chen, "A continuous asymptotic tracking control strategy for uncertain nonlinear systems," *IEEE Trans. Autom. Control*, vol. 49, no. 7, pp. 1206–1211, Jul. 2004.

[25] J. Yao, Z. Jiao, and D. Ma, "RISE-based precision motion control of DC motors with continuous friction compensation," *IEEE Trans. Ind. Electron.*, vol. 61, no. 12, pp. 7067–7075, Dec. 2014.

[26] W. Ji, A. Wang, and J. Qiu, "Decentralized fixed-order piecewise affine dynamic output feedback controller design for discrete-time nonlinear large-scale systems," *IEEE Access*, vol. 5, pp. 1977–1989, 2017.

[27] P. M. Patre, W. MacKunis, K. Kaiser, and W. E. Dixon, "Asymptotic tracking for uncertain dynamic systems via a multilayer neural network feedforward and RISE feedback control structure," *IEEE Trans. Autom. Control*, vol. 53, no. 9, pp. 2180–2185, Oct. 2008.

[28] N. Sharma, S. Bhasin, Q. Wang, and W. E. Dixon, "RISE-based adaptive control of a control affine uncertain nonlinear system with unknown state delays," *IEEE Trans. Autom. Control*, vol. 57, no. 1, pp. 255–259, Jan. 2012.

[29] N. Fischer, Z. Kan, R. Kamalapurkar, and W. E. Dixon, "Saturated RISE feedback control for a class of second-order nonlinear systems," *IEEE Trans. Autom. Control*, vol. 59, no. 4, pp. 1094–1099, Apr. 2014.

[30] W. Sun, H. Gao, and O. Kaynak, "Vibration Isolation for Active suspensions with performance constraints and actuator saturation," *IEEE/ASME Trans. Mechatronics*, vol. 20, no. 2, pp. 675–683, Apr. 2015.

[31] J. Yao, W. Deng, and Z. Jiao, "RISE-based adaptive control of hydraulic systems with asymptotic tracking," *IEEE Trans. Autom. Sci. Eng.*, vol. 14, no. 3, pp. 1524–1531, Jul. 2017.

[32] T. Wang and Q. Wang, "Modeling and control of a novel hydraulic system with energy regeneration," in *Proc. IEEE/ASME Int. Conf. Adv. Intell. Mechatronics*, Kachsiung, Taiwan, 2012, pp. 922–927.

CHENGYANG LUO received the B.Tech. degree from the North University of China, Taiyuan, China, in 2014. He is currently pursuing the Ph.D. degree with the School of Mechanical Engineering, Nanjing University of Science and Technology, Nanjing, China.

His current research interests include the nonlinear servo control of mechatronic systems, robotic and control.

JIANYONG YAO received the B.Tech. degree from Tianjin University, Tianjin, China, in 2006, and the Ph.D. degree in mechatronics from Beihang University, Beijing, China, in 2012. He was a Visiting Exchange Student with the School of Mechanical Engineering, Purdue University, from 2010 to 2011.

In 2012, he joined the School of Mechanical Engineering, Nanjing University of Science and Technology, Nanjing, China, and currently as a Full Professor. His current research interests include the servo control of mechatronic systems, adaptive and robust control, and the fault detection and accommodation of dynamic systems.

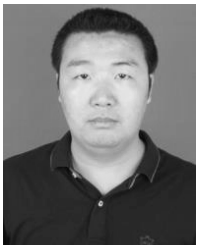

FUHONG CHEN received the B.Tech. degree from the School of Equipment Engineering, Shenyang Ligong University, Shenyang, China, in 2009, and the Ph.D. degree from the School of Mechanical Engineering, Nanjing University of Science and Technology, Nanjing, China, in 2014.

His current research interests include the servo control of mechatronic systems and robust adaptive control.

LAN LI received the master's degree in mechatronics from Beihang University, Beijing, China, in 2008. After that, she joined the Beijing Institute of Space Launch Technology, Beijing, and currently as a Senior Engineer. Her current research interests include the general design and servo control techniques of vehicle systems.

QIANG XU received the Ph.D. degree from the Nanjing University of Science and Technology, Nanjing, China, in 2000.

He is currently a Professor with the School of Mechanical Engineering, Nanjing University of Science and Technology. His current research interests include measuring technology and advanced thermal sensing technology.